*Electronic Materials Letters, Vol. 6, No. 3 (2010), pp. 91-95*
DOI: 10.3365/eml.2010.09.091 Published 30 September 2010

# Synthesis of $LiCo_{1/3}Ni_{1/3}Mn_{1/3}O_2$ by a Simple Combustion Method and Electrochemical Properties

**Hun Uk Kim,[1] Daniel R. Mumm,[2] Hye Ryoung Park,[3] and Myoung Youp Song[4,*]**

[1]Department of Chemical Engineering, Hangyang University,
17 Haengdang-dong, Seongdong-gu, Seoul, 133-791, Korea
[2]Department of Chemical Engineering and Materials Science,
University of California, Irvine CA 92697-2575, USA
[3]Faculty of Applied Chemical Engineering, Chonnam National University,
300 Yongbongdong Bukgu Gwangju, 500-757, Korea
[4]Division of Advanced Materials Engineering and Department of Hydrogen and Fuel Cells,
Hydrogen & Fuel Cell Research Center, Engineering Research Institute, Chonbuk National University,
664-14 1ga Deogjindong Deogjingu Jeonju Jeonbuk 561-756, Korea

$LiCo_{1/3}Ni_{1/3}Mn_{1/3}O_2$ was synthesized by a simple combustion method and its electrochemical properties were examined. The XRD patterns of the samples calcined at 900°C and 1,000°C showed sharp peaks for an $R\bar{3}m$ structure with clear splitting between the (006) and (102) peaks and between the (108) and (110) peaks. The size of the particles increased as the calcination temperature rose. The samples after combustion, and after combustion and calcinations, were analyzed by FT-IR. The samples calcined at 900°C and 1,000°C had similar a and c values, and similar first discharge capacities (176 mAh/g and 177 mAh/g, respectively, at 20 mA/g), but the sample calcined at 900°C had better cycling performance. The sample calcined at 900°C had smaller particles and more uniform particle sizes than the sample calcined at 1,000°C.

**Keywords:** $LiCo_{1/3}Ni_{1/3}Mn_{1/3}O_2$, a simple combustion method, electrochemical property, calcination temperature, $R\bar{3}m$ structure, cycling performance

## 1. INTRODUCTION

Lithium transition metal oxides, such as $LiCoO_2$,[1,2] $LiNiO_2$,[3-8] $LiMnO_2$,[9] and $LiMn_2O_4$,[10,11] have been investigated as cathode materials for rechargeable lithium batteries. Co-containing lithium oxide $LiCoO_2$ has been studied most intensively in order to develop commercial rechargeable batteries because the material has large diffusivity and a high operating voltage. However, cobalt is expensive and toxic. It has a layered structure ($R\bar{3}m$). Ni-containing lithium oxide $LiNiO_2$ with an $R\bar{3}m$ structure is considered a promising cathode material due to its large discharge capacity and low cost. However, due to the size similarity of Li and Ni ions ($Li^+$; 0.72 and $Ni^{2+}$; 0.69), $LiNiO_2$ is generally obtained in the non-stoichiometric composition $Li_{1-y}Ni_{1+y}O_2$[12,13] and the $Ni^{2+}$ ions in the lithium planes obstruct the movement of $Li^+$ ions during charging and discharging.[14,15] The Mn-containing lithium oxides, in which many researchers are interested, are $LiMnO_2$ and $LiMn_2O_4$. $LiMnO_2$ has an orthorhombic (Pmnm) structure and $LiMn_2O_4$ has a spinel (Fd3m) structure. Mn is chipper than Co and Ni. $LiMnO_2$ is not easy to synthesize, while $LiMn_2O_4$ is. However, $LiMnO_2$ has a theoretical charge-discharge capacity that is two times that of $LiMn_2O_4$. Many researchers have studied Mn-containing lithium oxides, but their cycling performances are not good because Jahn-Teller distortions cause deterioration of materials during charging and discharging.

Delmas *et al.*[16] classified $Na_yMnO_2$ into two groups; the O3, O1, O6 and P3 group, and the P2 and O2 group. The $MnO_2^{(-)}$ layers in the former group have the same directionality, but those in the latter group cross each other. Phase transition within the same group is possible by the sliding of a layer with the directionality of the layer maintained. Armstrong *et al.*[9] synthesized $LiMnO_2$ (O3, C2/m) by an ion exchange method and reported that this material has a very large first discharge capacity; however, the material is transformed into the spinel phase during the first discharge. The O2 layer structure is formed from the P2 structure. Paulsen *et al.*[17] synthesized $Li_{2/3}[Ni_{1/3}Mn_{2/3}]O_2$ with an O2 structure and reported that structural transformation does not occur in this material with charge-discharge cycling. However, this material has not been used to develop a cathode for practical commercial batteries since materials with the O2 structure

*Corresponding author: songmy@jbnu.ac.kr

are difficult to synthesize and have low discharge capacities at high current densities. Other researchers have investigated layered materials that do not undergo phase transitions during cycling in order to overcome the disadvantages of the the above transition metal-containing lithium oxides. Ohzuku *et al.*[18] synthesized $LiCo_{1/3}Ni_{1/3}Mn_{1/3}O_2$ and reported that it has a first discharge capacity of about150 mAh/g in the voltage range of 2.5 V to 4.2 V; also, it does not exhibit a structural transition during charging-discharging and is thermally stable. These properties have caused this material to attract interest as a possible replacement for $LiCoO_2$ in commercial lithium ion batteries.[19] For the synthesis of this material, a solid-sate reaction method is employed using starting materials with the hydroxide group[18,19] or using the mixed hydroxide method.[20] However, $Mn(OH)_2$ is hard to prepare and the control of synthesis conditions in the mixed hydroxide method is difficult. In addition, it is not easy to control the crystal structure, the purity or the physical properties of the synthesized material.[21]

In this work, in order to overcome the disadvantages of the synthesis methods studied previously, $LiCo_{1/3}Ni_{1/3}Mn_{1/3}O_2$ was synthesized by a simple combustion method. XRD, SEM, and FT-IR analyses were carried out and the electrochemical properties of the material were measured.

## 2. EXPERIMENTAL PROCEFURE

In order to synthesize $LiCo_{1/3}Ni_{1/3}Mn_{1/3}O_2$ by a simple combustion method, $Li(CH_3COO)\cdot 2H_2O$ (Aldrich Chemical Co. purity 98%), $Co(NO_3)_2\cdot 6H_2O$ (Aldrich Chemical Co. purity 98%), $Ni(NO_3)_2\cdot 6H_2O$ (Aldrich Chemical Co. purity 98%) and $Mn(CH_3COO)_2\cdot 4H_2O$ (Aldrich Chemical Co. purity 99+%) were used as starting materials. The starting materials in the desired composition were dissolved in distilled water. Materials were dried via continuous stirring with a magnetic stirrer on a hot plate until they became viscous, and were then combusted in air at 400°C for 30 min. Materials were then palletized and calcined in an oxygen stream at 400°C to 1,000°C for 10 h.

The phase identification of the synthesized samples was carried out by X-ray diffraction analysis using Cu $K_\alpha$ radiation. A Rigaku III/A X-ray diffractometer was used. The scanning rate was 6 $min^{-1}$ and the scanning range of the diffraction angle (2θ) was $10^\circ \le 2\theta \le 80^\circ$. The morphologies of the samples were observed with a scanning electron microscope (SEM, JEOL JSM-6400). FT-IR (Fourier-transform infrared) measurements were performed with the KBr method via an FT-IR spectrometer (ABB BOMEN MB100).

To measure the electrochemical properties, coin-shape cells (2016 type) were fabricated. The electrochemical cells consisted of the prepared sample as a positive electrode, Li metal as a negative electrode, and an electrolyte [Purelyte (Samsung General Chemicals Co., Ltd.)] prepared by solving1M $LiPF_6$ in a 1:1 (volume ratio) mixture of ethylene carbonate (EC) and diethyl carbonate (DEC). A Whatman GF/F glass fiber was used as a separator. The cells were assembled in an argon-filled dry box. To fabricate the positive electrode, active material, acetylene black and polyvinylidene fluoride (PVDF) binder with N-methyl-2-pyrrolidone (NMP) were mixed at a weight ratio of 90:6:4 on Al foil and dried at 80°C for 24 h. All the electrochemical tests were performed at room temperature with a battery charge-discharge cycle tester (galvanostatic measurement system) at 20 mA/g in a voltage range from 2.5 V to 4.5 V.

## 3. RESULTS AND DISCUSSION

Figure 1(a) shows the XRD patterns of the $LiCo_{1/3}Ni_{1/3}Mn_{1/3}O_2$ after combustion and after being calcined at 400, 500, 600, and 700°C for 10 h after combustion; Fig. 1(b)

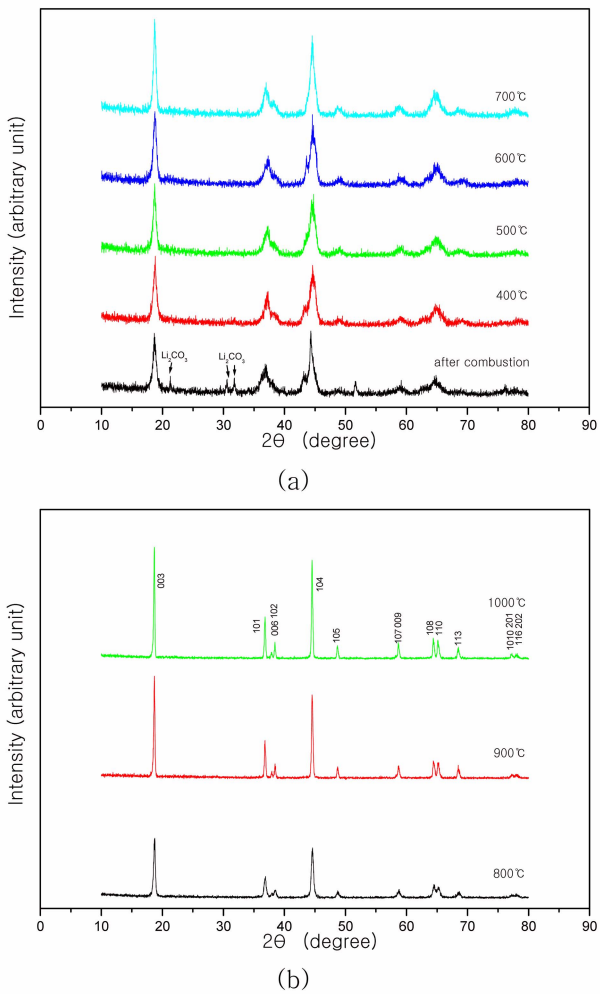


**Fig. 1.** XRD patterns of $LiCo_{1/3}Ni_{1/3}Mn_{1/3}O_2$ (a) after combustion, and after being calcined at 400°C, 500°C, 600°C, and 700°C for 10 h after combustion, and (b) after being calcined at 800°C, 900°C, and 1,000°C for 10 h after combustion.

shows the XRD patterns after being calcined at 800°C, 900°C, and 1,000°C for 10 h after combustion. Figure 1(a) shows peaks corresponding to an $R\bar{3}m$ structure. The XRD pattern after combustion gives the peaks for $Li_2CO_3$ as well. The peaks for $Li_2CO_3$ do not appear after calcination at or above 400°C for 10 h. Figure 1(b) shows peaks corresponding to an $R\bar{3}m$ structure. As the calcination temperature increases, the peaks become sharper, indicating that the crystallinity of the formed phase increases. The sample calcined at 800°C does not show distinct splitting between the 006 and 102 peaks or between the 108 and 110 peaks. However, the samples calcined at 900°C and 1,000°C exhibit clear splitting between the 006 and 102 peaks and between the 108 and 110 peaks. The samples calcined at 900°C and 1,000°C have similar a and c values (at 900°C, $a$ = 2.859 Å, $c$ = 14.241 Å; at 1,000°C, $a$ = 2.860 Å, $c$ = 14.241 Å). The appropriate calcination temperature was thus considered equal to or higher than 900°C.

Microstructures derived by SEM of $LiCo_{1/3}Ni_{1/3}Mn_{1/3}O_2$ (a) after combustion, and after being calcined at (b) 400°C, (c) 500°C, (d) 600°C, (e) 700°C, (f) 800°C, (g) 900°C and (h) 1,000°C for 10 h after combustion are presented in Fig. 2. The sample after combustion has a microstructure similar to dumps covered with very small branches. The samples calcined after combustion have microstructures very different from those of the sample just after combustion. All the samples have spherical particles and the particles are agglomerated. The size of particles increases as the calcination temperature rises. The sample calcined at 1,000°C has relatively large particles.

Figure 3 gives the FT-IR graph of $LiCo_{1/3}Ni_{1/3}Mn_{1/3}O_2$ after combustion at 400 for about 30 min. Peaks at 443 $cm^{-1}$, 420 $cm^{-1}$, and 401 $cm^{-1}$, peaks at 540 $cm^{-1}$and 505 $cm^{-1}$, and peaks at 2,364 and 2,345 $cm^{-1}$ are considered to correspond to O-M-O bonds. The broad peak at 650-590 $cm^{-1}$ is also considered to correspond to the O-M-O bond. In addition, peaks reported to correspond to $Li_2CO_3$ are observed at 1,500 $cm^{-1}$, 1,438 $cm^{-1}$, and 864 $cm^{-1}$. The peaks at 1,300 $cm^{-1}$ to 1,000 $cm^{-1}$, 1,750 $cm^{-1}$ to 1,630 $cm^{-1}$, 2,900 $cm^{-1}$ to 2,700 $cm^{-1}$, and 3,400 $cm^{-1}$ to 3,200 $cm^{-1}$ are deemed to be indicative of the C-O bond, C=O bond, $CH_3$ bond and O-H bond, respectively; they are considered to correspond to acetic acid $CH_3COOH$. It is thus considered that the sample after combustion is in a state of a mixture consisting of $MO_n$ and acetic acid, and that the acetic acid does not decompose completely even after combustion.

The FT-IR graph of $LiCo_{1/3}Ni_{1/3}Mn_{1/3}O_2$ after combustion at 400 for about 30 min and of those calcined at various temperatures for 10 h after combustion is shown in Fig. 4. As the calcination temperature increases, the intensities of the $Li_2CO_3$ peak and the O-M-O bond peaks (at 505 $cm^{-1}$ and at 443 $cm^{-1}$, 420 $cm^{-1}$ and 401 $cm^{-1}$) decrease. The peak at 540 $cm^{-1}$ and the broad peak at 650 $cm^{-1}$ to 590 $cm^{-1}$ corresponding to the O-M-O bonds become stronger, and they shift toward lower wavenumbers as the calcination temperature increases.

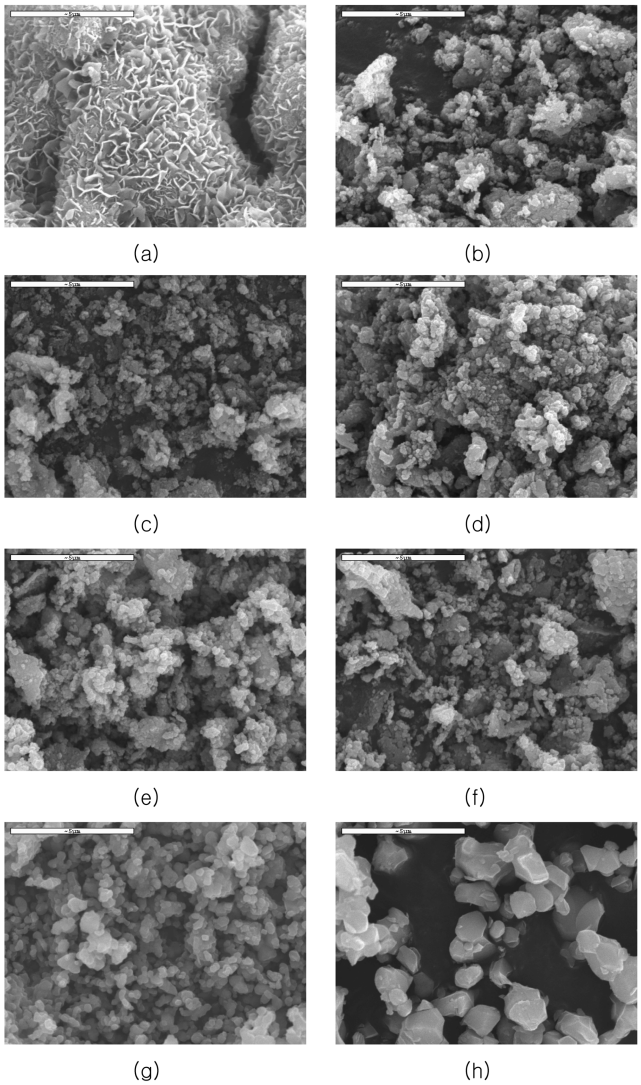


**Fig. 2.** Microstructures by SEM of $LiCo_{1/3}Ni_{1/3}Mn_{1/3}O_2$ (a) after combustion, and after being calcined at (b) 400°C, (c) 500°C, (d) 600°C, (e) 700°C, (f) 800°C, (g) 900°C, and (h) 1,000°C for 10 h after combustion.

Figure 5 presents variations of the discharge capacity at 20 mA/g (voltage range 2.5 V to 4.5 V) with the number of charge-discharge cycles for the $LiCo_{1/3}Ni_{1/3}Mn_{1/3}O_2$ calcined at 800°C, 900°C, and 1,000°C for 10 h after combustion. The sample calcined at 800°C has a low first discharge capacity (139 mAh/g) and a poor cycling performance. The samples calcined at 900°C and 1,000°C have high first discharge capacities (176 mAh/g and 177 mAh/g, respectively) and better cycling performances than that of the sample calcined at 800°C. The values of a and c for the samples calcined at 900°C and 1,000°C are similar, but the cycling performance of the sample calcined at 900°C is better than that of the sample calcined at 1,000°C. The particles of the sample cal-

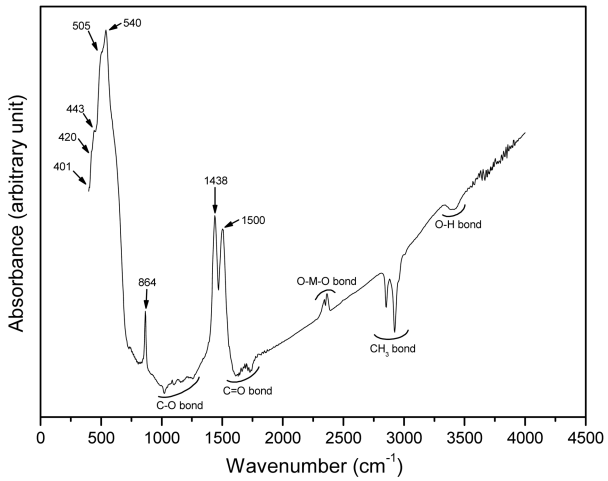


**Fig. 3.** FT-IR graph of $LiCo_{1/3}Ni_{1/3}Mn_{1/3}O_2$ after combustion.

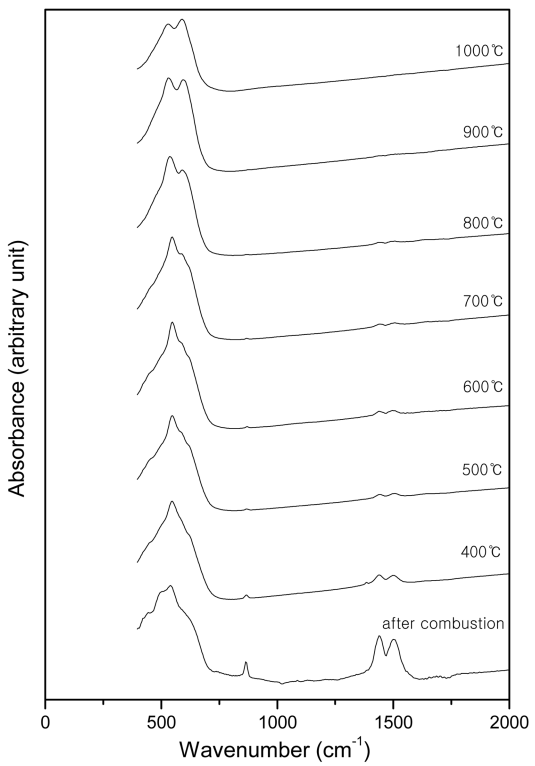


**Fig. 4.** FT-IR graph of $LiCo_{1/3}Ni_{1/3}Mn_{1/3}O_2$ after combustion, and after being calcined at various temperatures for 10 h after combustion.

cined at 900°C are smaller and more uniform in size than those of the sample calcined at 1,000°C. The cycling performance is probably related to the particle size and the uniformity of particle size of the sample. The first discharge capacities (176 mAh/g and 177 mAh/g, respectively) of the $LiCo_{1/3}Ni_{1/3}Mn_{1/3}O_2$ samples calcined at 900 and 1,000 are larger than that of the $LiCo_{1/3}Ni_{1/3}Mn_{1/3}O_2$ sample (about150 mAh/g in the voltage range of 2.5 V to 4.2 V) synthesized by

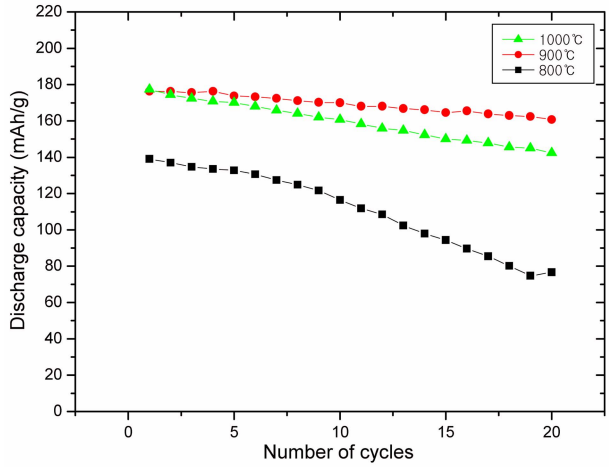


**Fig. 5.** Variations of the discharge capacity at 20 mA/g (voltage range 2.5 V to 4.5 V) with the number of charge-discharge cycle for $LiCo_{1/3}Ni_{1/3}Mn_{1/3}O_2$ calcined at 800°C, 900°C, and 1,000°C for 10 h after combustion.

the solid-sate reaction method.[18] This is believed to be partly thanks to a homogeneous mixing of the starting liquid materials for the preparation of the samples in the simple combustion method.

## 4. CONCLUSIONS

$LiCo_{1/3}Ni_{1/3}Mn_{1/3}O_2$ was synthesized by a simple combustion method and its electrochemical properties were examined. The XRD patterns of the samples calcined at 900°C and 1,000°C exhibited the sharp peaks of an $R\bar{3}m$ structure. The samples after combustion were in a state of a mixture consisting of $MO_n$ and acetic acid. As the calcination temperature increased, the intensity of the $Li_2CO_3$ peak decreased while the intensities of the peak at 540 $cm^{-1}$ and the broad peak at 650 $cm^{-1}$ to 590 $cm^{-1}$ corresponding to O-M-O bonds became stronger. The samples calcined at 900°C and 1,000°C had similar a and c values and similar first discharge capacities (176 mAh/g and 177 mAh/g, respectively, at 20 mA/g), but the sample calcined at 900°C had better cycling performance. The sample calcined at 900°C had smaller particles and more uniform particle sizes than the sample calcined at 1,000°C.

## REFERENCES

1. K. Ozawa, *Solid State Ionics* **69**, 212 (1994).
2. Z. S. Peng, C. R. Wan, C. Y. Jiang, *J. Power Sources* **72**, 215 (1998).
3. J. R. Dahn, U. von Sacken, M. W. Juzkow, H. Al-Janaby, *J. Electrochem. Soc.* **138**, 2207 (1991).
4. M. Y. Song, R. Lee, *Solid State Ionics* **111**, 97 (2002).
5. J. G. Lee, C. J. Kim, B. S. Kim, D. Y. Son, and B. W. Park,

*Electron.Mater. Lett*. **2**, 111 (2006).
6. H.-S. Kim, K.-T. Kim, and P. Periasamy, *Electron. Mater. Lett*. **2**, 119 (2006).
7. Y. H. Oh, D. G. Ahn, S. H. Nam, C. J. Kim, J. G. Lee, and B. W. Park, *Electron. Mater. Lett.* **4**, 103 (2008).
8. M. Y. Song, C. K. Park, S. D. Yoon, H. R. Park, and D. R. Mumm, *Electron. Mater. Lett.* **4**, 151 (2008).
9. A. R. Armstrong and P. G. Bruce, *Nature* **381**, 499 (1996).
10. J. M. Tarascon, E. Wang, F. K. Shokoohi, W. R. Mckinnon, and S. Colson, , *J. Electrochem. Soc.* **138**, 2859 (1991).
11. M. Y. Song and D. S. Ahn, *Solid State Ionics* **112**, 245 (1998).
12. P. Barboux, J. M. Tarascon, and F. K. Shokoohi, *J. Solid State Chem.* **94**, 185 (1991).
13. J. Morales, C. Perez-Vicente, and J. L. Tirado, *Mater. Res. Bull.* **25**, 623(1990).
14. A. Rougier, I. Saadoune, P. Gravereau, P. Willmann, and C. Delmas, *Solid State Ionics* **90**, 83 (1996).
15. B. J. Neudecker, R. A. Zuhr, B. S. Kwak, and J. B. Bates, *J. Electrochem. Soc.* **145**, 4161 (1998).
16. C. Delmas, J. -J. Braconnier, A. Maazaz, and P. Hagenmuller, *Rev. Chim. Miner.* **19**, 343 (1982).
17. J. M. Paulsen, C. L. Thomas, and J. R. Dahn, *J. Electrochem. Soc.* **146**, 3560 (1999).
18. T. Ohzuku and Y. Makimura, *Chem. Lett.* 642 (2001).
19. N. Yabuuchi and T. Ohzuku, *J. Power Sources* **119-121**, 171 (2003).
20. Z. Lu, D. D. MacNeil, and J. R. Dahn, *Electrochem. Solid-State Lett.* **4**, A191 (2001).
21. H. Ito, M. Shimakawa, T. Tanaka, T. Ohzuku, 5th Hawaii Battery Conference, Waikaloa, HI (2003).